Optimization Study for Treatment of Acid Mine Drainage Using Membrane Technology

H. Al-Zoubi[a]; A. Rieger[b]; P. Steinberger[b]; W. Pelz[c]; R. Haseneder[b]; G. Härtel[b]

[a] Department of Chemical Engineering, Al-Hussein Bin Talal University, Ma'an, Jordan [b] Department of Environmental Process Engineering, Freiberg University of Mining and Technology, Germany [c] Siemens AG Industry Sector I IS MT MI, Erlangen, Germany

PLEASE SCROLL DOWN FOR ARTICLE

Taylor & Francis
Taylor & Francis Group

Optimization Study for Treatment of Acid Mine Drainage Using Membrane Technology

H. Al-Zoubi,[1] A. Rieger,[2] P. Steinberger,[2] W. Pelz,[3] R. Haseneder,[2] and G. Härtel[2]

[1]*Department of Chemical Engineering, Al-Hussein Bin Talal University, Ma'an, Jordan*
[2]*Department of Environmental Process Engineering, Freiberg University of Mining and Technology, Germany*
[3]*Siemens AG Industry Sector I IS MT MI, Erlangen, Germany*

The use of membrane technology in the treatment of Acid Mine Drainage (AMD) can result in reduction of chemical usage and sludge production making the treatment process more environmentally friendly. This study deals with the optimization of membrane filtration performance in the treatment of AMD using two nanofiltration (NF) membranes (NF99 and DK) and one reverse osmosis (RO). All membranes were used in various tests treating a model solution at two different concentration levels in order to cover the concentration of actual AMD found in the mining industry. The main parameters which were studied to determine the optimal condition for AMD filtration are pressure, pH, temperature, and flow rate. Pressure and temperature were found to have a considerable influence on flux, while rejection was only slightly influenced by pressure. The feed flow rate had no effect on rejection. The highest flux with moderate rejection was determined for NF99 while RO had the lowest flux but highest rejection. Therefore, NF is preferable for AMD treatment due to lowest energy consumption. The treatment has also been tried on a large scale to check its applicability at a commercial scale. Finally, PHREEQC has been used to determine the scaling risk in the prepared AMD.
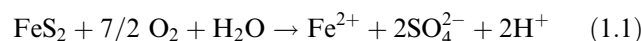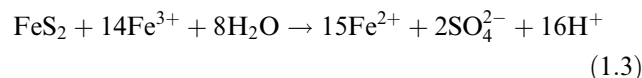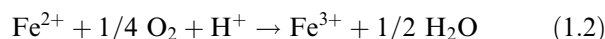
INTRODUCTION

Acid mine drainage (AMD) is characterized by high acidity with pH values in the range of 2 to 4, high sulphate concentration (1–20 g/L), and high concentrations of metals and other toxic elements such as Fe, Mn, Al, Cu, Ca, Pb, Mg, Na, and Ni (1,2). Even though many acidic mine waters fit into the range of pH 2 to 4, there are also extreme mine waters. As an example, Nordstrom et al. (3) report a mine water from an Iron Mine in California, Richmond Mine at Iron Mountain, CA, USA. The mine waters that evolve from that mine are characterized by sulphate contents as high as 760 g/l, 200 mg of total dissolved metals,

and a pH of −3.6 (3). All these properties of mine waters (pH, sulphate content, toxic metals content) cause a severe contamination of surface and groundwater as well as soils.

AMD results from the natural oxidation of sulphide minerals, such as pyrite (FeS_2), mackinawite (FeS) and chalcocite (Cu_2S), when exposed to the combined action of water and oxygen as shown in the following reactions (4). Equation (1.1) describes the direct oxidation of pyrite in an oxic environment.

$$FeS_2 + 7/2\ O_2 + H_2O \rightarrow Fe^{2+} + 2SO_4^{2-} + 2H^+ \quad (1.1)$$

Depending on the availability of a sufficiently acidic and oxidizing environment supported by microorganisms such as *Acidithiobacillus ferroxidans* the produced ferrous iron is oxidized to ferric iron, which subsequently oxidizes pyrite according to Eq. (1.3) or forms insoluble ferric iron hydroxide according to Eq. (1.4) Both reactions produce acidity that can be held responsible for leaching (toxic) metals from the ambient rocks.

$$Fe^{2+} + 1/4\ O_2 + H^+ \rightarrow Fe^{3+} + 1/2\ H_2O \quad (1.2)$$

$$FeS_2 + 14Fe^{3+} + 8H_2O \rightarrow 15Fe^{2+} + 2SO_4^{2-} + 16H^+ \quad (1.3)$$

$$Fe^{3+} + 3H_2O \rightarrow Fe(OH)_3(s) + 3H^+ \quad (1.4)$$

According to Akcil and Koldas (4), the combination of reactions (1.1, 1.2) and (1.4) leads to a more simplified scheme, that is shown in Eq. (1.5) and summarizes acid generation, pyrite oxidation, and precipitation of $Fe(OH)_3$. The accumulation of ferric hydroxide represents an unavoidable by-product of the mining and mineral industries and one of the significant contributors to water pollution.

$$FeS_2 + 15/4\ O_2 + 7/2H_2O \rightarrow Fe(OH)_3(s) + 2SO_4^{2-} + 4H^+ \quad (1.5)$$

Different conventional methods were used in treating AMD. Lime $(Ca(OH)_2)$ or limestone $(CaCO_3)$ neutralization is a traditional approach used by many investigators (5–9), in which lime or limestone is added to precipitate the sulphate as gypsum and metals as hydroxides followed by gravity separation of the solid product thereby raising the pH. This process generates large amounts of gypsum sludge contaminated with toxic metals, and is also expensive and labor intensive. In South Australia, the capital cost of this treatment was estimated at \$250,000/year in 1988 (10). Moreover, the remaining sulphate content is still about 1440 mg/l of sulphate according to the gypsum solubility equilibrium. Based on the complex composition of mine waters this residual content of sulphate can be reduced when more complex mineral phases of metals will be precipitated at higher pH values. Still the residual content (for SO_4^{2-} in case of gypsum equilibrium of about 1440 mg/l) exceeds or would exceed the environmental requirements for such water going to the receiving bodies. Many researchers tried different chemicals in stead of limestone for neutralization of AMD (11–20). Feng et al. (13) used a blast furnace slag instead of limestone. The authors showed that this process has the potential to absorb metal ions with increased pH to neutral. On the other hand, Petrik et al. (14) showed that it was possible to use fly ash or fly ash leachate as an alternative agent in neutralization of AMD without the addition of a liming agent. Maree et al. (15) used barium chloride and barium sulphide to precipitate barium sulphate thus removing metals and sulphate from mine waters. While the final sulphate content using lime treatment is about 1440 mg/l, this method can reduce sulphate content using combined BaSO4 and BaS treatment to about 200 mg/l (15). A disadvantage of this process is the high security measures due to treatment with a toxic element such as barium, which is from the authors point of view the main reason, why this method is not that widely used.

Biological treatment is another conventional method used for treatment of AMD in which sulphate-reducing bacteria (SRB) are used to remove metals and raise the pH value. These reactors commonly use a variety of carbon substances (i.e., manure, wood chips) to reduce sulphate to sulphide, which forms metal sulphide precipitates (21–25). This process for some typical organic materials generates hydrogen sulphide and alkalinity as bicarbonate resulting from organic substrate metabolization. The formation of hydrogen sulphide causes immobilization of solved metals by precipitation of metal sulphides, while the formed bicarbonate neutralizes the acid. The pH increase subsequently followed by neutralization causes also a metal hydroxide precipitation by hydrolysis followed by a competitive acidification-neutralization cycle that involves bicarbonate (25). The effectiveness of these methods decreases as carbon substances are consumed in the SRB reactor.

Therefore, Barnes et al. (26) suggested using lactic acid and methanol as a carbon source in a similar sulphate-reducing bioreactor process.

The cation exchange process is another potential method used to treat AMD (27). Not only would ion exchangers remove potentially toxic metals from mine runoff, there was also the possibility of making a profit from the recovered metals. However, the cost of ion exchange materials compared to the possible returns, as well as the inability of current technology to efficiently deal with the vast amounts of mine discharge, renders this solution unrealistic at present.

Membrane technology is an efficient alternative method used to treat AMD. Nanofiltration (NF) membranes have been established in our previous work, which showed very promising results in treating AMD (28). In that work, high rejections of toxic metals dissolved in AMD based on the total electrical conductivity have been obtained at different concentration levels and at pressures of 20 (2 MPa) and 30 bar (3 MPa). These data encouraged us to study all parameters such as pressure, feed flow rate, temperature, pH, and concentration that optimize the treatment of AMD. Reverse osmosis (RO) will also be conducted in this work for a comparison target. NF offers several advantages over other types of membranes, such as low operation pressure, high flux, high retention of multivalent anion salt and organic molecules above 300 Dalton, relatively low investment, low operation and maintenance cost, and is environmentally friendly (28–29).

In previous studies, the effect of different parameters (pressure, concentration, temperature, and pH) on the separation efficiency of NF has been investigated. Many researchers studied the effect of pressure and concentration on the rejection of different salts as a single phase (30–31) and as a mixture phase (32–33) using different types of NF membranes. The results showed that the rejection increases with increasing pressure and decreasing concentration, which could be explained on the basis of steric hindrance mechanism, which is consistent with findings derived from the AFM characterization (30). On the other hand, the effect of temperature on the salt rejection through NF membranes has been investigated by Snow et al. (34). The authors concluded that the increase in salt permeation (low rejection) and water flux with increasing temperature was found to be approximately the same at constant pressure due to the higher activation energy of the salt solution in comparison to pure water. Nilsson et al. (35) explained the later findings by polymer reorientation of the membrane due to an increase in flexibility of the molecular chains with increasing temperature. The increase in temperature causes decrease in viscosity, reduces the pressure drop, and increases the external mass transfer (lower concentration polarization) (36). pH is another important factor in studying the rejection of salt solutions since it

affects the NF separation performance to a great extent. It has an effect on the surface charge of the membrane due to the disassociation of functional groups. Zeta potential, which is used to quantify the membrane surface charge, has been observed to become increasingly more negative for most membranes as pH is increased (37). Therefore, an increase in the surface charge of the membrane results in increased electrostatic repulsion between a negatively charged solute and the membrane. On the other hand, the presence of counterions such as Ca^{2+}, Na^+, Mg^{2+}, Cu^{2+}, and K^+ in feed water was reported to reduce the negative zeta potential of the membrane (38).

Separations of single metal ions as well as binary metal solutions (39) using membrane technology were reported in the literature, but the same on mixtures of metals is feeble. This experimental investigation deals with the separation of ions from a model water referring to an AMD that has been provided by SIEMENS AG, Erlangen Germany. Its composition can be found in Table 1. The main focus of this work was to study the effect of pressure, concentration, temperature, and pH on the rejection of dissolved metals and sulphate from artificial AMD solution using two types of NF membranes and one type of RO. This will highlight the optimized parameters, which should be followed in the treatment of AMD using membrane technology. The synthetic AMD was prepared in our laboratory at two concentration levels, as shown in Table 1, in order to cover the range of the concentration of some actual AMD in the mining industries. PHREEQC has been used to find the expected precipitation, which may be formed during the preparation and treatment of AMD. Finally, the rejection of the main components dissolved in AMD and flux decline will be investigated

using a disc tube NF99 module with an area of about $6\,m^2$ at two pH values.

THEORY

United States Geological Survey (USGS) PHREEQC 2.1 is a software tool, which can be used to determine the scaling risk in an aqueous solution. It is based on calculations of solubility equilibria of ions and the use of thermodynamic data from a database file, that can be selected by the user (40). The software includes a wide variety of aqueous geochemical calculations at ambient temperature based on mass and energy conservation and transport equations, and kinetic approaches and has many more capabilities, which are not mentioned here, but can be found in the manual (41). As for the results, the software provides a complete scheme of ion speciation based on the database file and the analytical input data. The input data includes temperature, pH, redox potential or redox couples, and analytical data of the solution composition. Based on speciation data and solubility calculations, the main inorganic constituents of an aqueous solution are listed by mineral phases and completed with a saturation index (41). This saturation index is calculated using Eq. (2).

$$SI = \log(\Pi a_i^{\nu}/K_T) \qquad (2)$$

Where SI is the saturation index, Πa_i the ion activity product, ν the stoichiometric factor of the relevant ion, and K_T the solubility product of an inorganic compound. As the SI is defined as a logarithmic parameter, the saturation factor (SF) is another parameter calculated using equations (3.1–3.2) (41). The latter factor gives a better idea of the magnitude, but due to the missing indication of

TABLE 1
The ions concentration of the investigated synthetic and real AMD

Ions	Synthetic AMD at low concentration (mg/l) pH = 2.37	Synthetic AMD at high concentration (mg/l) pH = 2.46	Actual AMD solution (mg/l) pH = 2.50 (28,44)
Al^{3+}	648 (760*)	1295 (1290*)	1139.0
SO_4^{2-}	13429 (9400*)	26858 (20400*)	14337
Ca^{2+}	221 (240*)	441 (395*)	325.9
Cu^{2+}	1399 (1680*)	2797 (2735*)	2298.0
Fe^{3+}	501 (300*)	1002 (446*)	627.5
Mn^{3+}	135 (162*)	271 (295*)	224.5
Mg^{2+}	394 (482*)	789 (776*)	630.60
Na^+	N/A	N/A	6.89
K^+	N/A	N/A	4.31
CO_3^{2-}	660 (N/A*)	1320 (N/A*)	N/A
TDS** (mg/l)	17387	34773	19594

*this value was measured experimentally, N/A: not available, **total dissolved solids.

supersaturation or undersaturation it is no longer commonly used.

$$SF = 10^{SI} \quad \text{for SI} > 0 \tag{3.1}$$

$$SF = 10^{[SI]} \quad \text{for SI} < 0 \tag{3.2}$$

The inorganic constituent is undersaturated when SI is lower than zero, supersaturated when SI is higher than zero, and when SI equals zero the inorganic constituent of interest is in solubility equilibrium. The SF gives a non-logarithmic number that equals the ratio between the ion activity product and the solubility product.

For simplicity, the concentration polarization was neglected in this study; therefore, the rejection (R) was calculated either for AMD solution or for ions using the following equation:

$$R = 1 - (C_p/C_f) \tag{4}$$

Where C_p and C_f are permeate and feed concentrations (mg/l) respectively. The flux ($L.h^{-1}.m^{-2}$) was also calculated as:

$$\text{Flux} = V_p/(t.A) \tag{5}$$

Where V_P is the volume of the collected permeate (L), t is time (h), and A is effective membrane filtration area (m^2).

EXPERIMENTAL
Membranes

Three commercial membranes were used in this study, of which one was manufactured by GE-Osmonics (USA). This is a thin-film-composite (TFC) NF membrane (DK). The second membrane is also a NF membrane (NF 99) obtained from Alfa Laval (Sweden), which was made as polyamide thin film (TF) composite on polyester. Finally, the third membrane is a RO membrane (HR98PP) which

is also obtained from Alfa Laval and made as TF composite. The data of all investigated membranes given by the manufacturers in addition to some values taken from the literature are shown in Table 2. All membranes were immersed in deionized water for at least one hour before being used in any experimental work.

Permeation Experiments and Set-Up

The permeation experiments were carried out in a laboratory-scale test cell at two different sizes; small and large. A schematic diagram of the small-scale experimental set-up has been described elsewhere (28). It mainly consists of a 30 liter feed tank, a high performance piston pump, two parallel test cells, a water bath, and a control unit. Twenty-five liters of the AMD feed were pumped using a Cat 1051 plunger pump into a junction, which distributes the flow equally to the two membrane cells. Each cell consists of a sinter plate to support a circular area membrane sample with an effective membrane area of 63.6 cm^2. The control unit in the set-up tracked the parameters such as pressure, flow, and temperature at required values. Two experiments, therefore, were carried out in a cross-flow NF membrane process at the same time using either the same or different types of membranes. The trans-membrane pressure and volumetric flow rate were adjusted using the concentrate (reject) outlet valve. The experiments were carried out in total re-circulation mode, i.e., both the concentrate and the permeate streams are re-circulated into the feed tank, so that the feed concentration is kept approximately constant. Effects of feed flow rate (900, 800, 700, 600, 500, and 400 L/h), temperature (60, 50, 40, 30, 20°C), and feed pressure (20, 17, 14, 11, 8, and 5 bar; 2, 1.7, 1.4, 1.1, 0.8, 0.5 MPa) were studied on the permeate flux and rejection of main components dissolved in AMD for all investigated membranes at low and high concentration levels. The pH was adjusted using 1 M H$_2$SO$_4$ p.a. (Merck Germany), and the temperature of the feed solutions was controlled using a thermostat water bath.

TABLE 2

Chemical and physical characteristics of NF and RO membranes taken from literature or supplied by the manufacturers

Membrane	NF 99	DK	RO (HR98PP)
Manufacturer	Alfalaval	GE-Osmonics	Alfalaval
Surface material	TF composite on polyester	TFC	TF composite on polypropylene
Temperature resistance (°C)	50	90	60
pH range (25°C)	2–10	2–11	2–10
Permeability (L/(m^2 h bar)) (20°C)	N/A	5.0 (37)	N/A
Rejection-size	>98 – MgSO$_4$	98 – MgSO$_4$	>96% – NaCl*

N/A: Not Available, *: based on 0.2% solution, 16–40 bar, 25°C.

The permeate flux was calculated for each experiment by measuring manually the time required to collect a specific volume of permeate divided by the surface area of investigated membranes.

The large scale set-up used in this study is shown in Fig. 1. It is a Disc Module type MD 12 of Envirochemie GmbH, Germany, with a relatively large area of about $6 \, m^2$. Compared to the small scale set-up, there are two major modifications: The two small circular modules were replaced with a disc tube module and the feed volume was increased to 80 liters. In the large-scale tests, the flux decline with time and the rejection of main components dissolved in AMD at two pH values of 1.5 and 2.4, and pressure in the range of 10 to 30 bar (1 to 3 MPa) has been studied. These investigations have been performed for a first insight on AMD membrane filtration in a commercial scale.

Sampling and Analytical Methods

In this study, a synthetic AMD has been prepared and filtered at two different concentration levels in order to cover the range of the concentration of actual AMD found in the mining industries. Table 1 shows the concentration of anions and cations of the synthetic AMD at low and high concentration levels. Both concentration levels differ by a factor of approximately 2. It is elucidated that the actual concentration of AMD, which was collected from a Chilean mining site and analyzed in our previous study (28), is among the two investigated concentration levels as shown in Table 1. The remaining cations such as (Na^+, K^+) have been neglected in the synthetic AMD for the reason that their concentrations are comparably low (11 mg/l). The synthetic AMD, in this study, has been prepared from typical chemicals such as $Al_2(SO_4)_3$, $CaCO_3$, $CuSO_4$, $Fe_2(SO_4)_3$, $MnSO_4$, and $MgSO_4$ which give similar ions found in the actual AMD. In order to remove large particles from the original AMD solution, it was filtered through a paper filter (Filtrak 388; Spezialpapierfabrik Niederschlag, Germany). The carbonate concentration

was not considered in this study as its value is very low at low pH due to its reaction with H_2SO_4. More details about the carbonate ions will be shown in the next section.

In order to determine the general rejection of the main components dissolved in AMD for each investigated NF membrane, the electrical conductivity for the feed and permeate solutions were measured at ambient temperature by a hand-held conductivity meter LF 330/340 (WTW-Germany) with electrical conductivity auto-correction to a temperature of 25°C, while the pH values were measured using a pH 340 meter (WTW, Germany). All cation concentrations were determined using inductively coupled plasma-optical emission spectroscopy (ICP-OES) with OPTIMA 3000 (Perkin-Elmer-USA). The sulphate concentrations were measured by an optical method using both test kits LCK 153 and LCK 353 (HACH-LANGE, Germany) to measure sulphate ions over the ranges 40–150 mg/l and 150–900 mg/l, respectively.

RESULTS AND DISCUSSIONS
PHREEQC

The ion compositions for the synthetic AMD at two concentration levels shown in Table 1 are used as an input data for PHREEQC (40) calculations in order to find the expected main scalants in the AMD. Even though there are many database files included in the installation package of PHREEQC (40), which provide much more data like the files phreeqc.dat or wateq4f.dat, the authors decided to use wateq4f.dat since a test with the other database files show only marginal differences in the calculated saturation indexes. These scalants are mainly gypsum, metal hydroxides (amorphous $Fe(OH)_3$, $Al(OH)_3$, $Mn(OH)_2$), and metal oxyhydroxides (FeOOH and MnOOH). Table 3 summarizes the results of SI and SF for both synthetic AMD solutions under study. According to these results, it is elucidated that there is no scaling of metal hydroxides and oxyhydroxides due to the high value of SI in negative and solubility equilibria of the tested metal compounds, which strongly depend on pH. According to Stumm and Morgan (42), redox-potential-pH-predominance data indicates no precipitation of ferric iron and aluminium (oxy)hydroxides and manganese (oxy)hydroxides for pH < 3. According to the PHREEQC (40), calculations all metal (oxy) hydroxides are undersaturated. Ferric iron as Goethite shows the lowest undersaturation compared to the other inorganic constituents, which is clearly related to the hydrolysis equilibrium with a pK_L close to the solution pH, while all the other hydroxides show undersaturation with orders of magnitude from 6 to 17. Gypsum solubility does not depend on pH in a comparable measure. The calculation results for gypsum indicate a state near the solubility equilibrium with a slight undersaturation for the synthetic AMD with low concentration and a slight
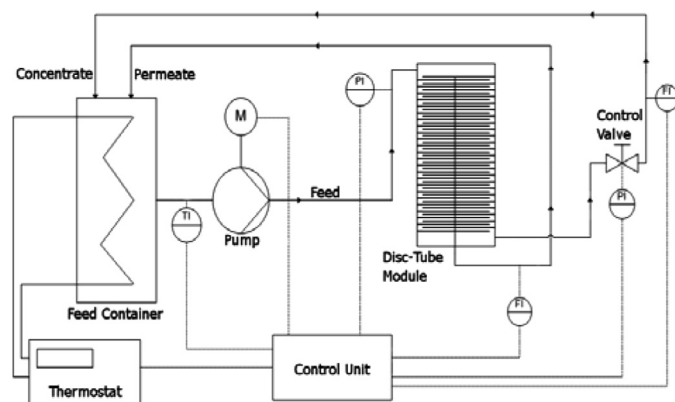

FIG. 1.   Disc tube module experimental set up.

TABLE 3
Saturation Index (SI) saturation factor (SF) for the investigated synthetic AMD determined by PHREEQC (40) using wateg4f.dat thermodynamic database at pH 2.4 and 20°C

Precipitates	Mineral phase	Synthetic AMD (low concentration)		Synthetic AMD (high concentration)	
		SI	SF	SI	SF
$(CaSO_4 \cdot 2H_2O)$	Gypsum	−0,21	1,62 (u*)	0,16	1,45 (s**)
$Fe(OH)_3$	(amorphous)	−9,8	$6,3*10^9$ (u)	−9,3	$2,0*10^9$ (u)
$Al(OH)_3$	(amorphous)	−7,8	$6,3*10^6$ (u)	−7,5	$3,2*10^7$ (u)
$Mn(OH)_2$	Pyrochroite	−13,9	$7,9*10^{13}$ (u)	−13,5	$3,2*10^{13}$ (u)
FeOOH	Goethite	−4,1	$1,3*10^4$ (u)	−3,6	$3,9*10^3$ (u)
MnOOH	Manganite	−17,6	$3,9*10^{17}$ (u)	−17,2	$1,6*10^{17}$ (u)

*u: undersaturated, and **s: supersaturated.

supersaturation for the synthetic AMD with high concentration, respectively. Comparing the calculated and the analytical data for the synthetic AMD composition as shown in Table 1, a decrease in concentration of calcium and sulphate content has been determined. This indicates a precipitation to the state near the solubility equilibrium of gypsum during the model water preparation. Carbonate, which has been added to the model water as calcium carbonate to increase water hardness, has been neglected in saturation calculations because of the low solution pH. As is well known from basic equilibrium chemistry, carbonate does not exist at pH lower than 6, but is transformed into CO_2, H_2CO_3, and highly soluble bicarbonate according to the carbonic acid equilibrium (42). Therefore, the carbonate ion is neglected in the analyzing process of AMD as shown in Table 1. Moreover, the scaling causing the efficiency reduction of the membrane process, is based on the precipitation of gypsum, but not on precipitation of metal (oxy) hydroxides or carbonates. A risk of colloidal fouling caused by metal hydroxide precipitation can be neglected for all the named metals, besides Goethite that might precipitate, when the solution pH is increased by 0.5 to 1 pH unit.

Pure Water Permeability of the Membranes

Pure water flux for all investigated membranes was found to increase linearly with the transmembrane pressure, with all curves passing through the origin in accordance with the null value of the osmotic pressure. Figure 2 shows that the water flux for NF99 membranes was the highest among the studied membranes under all pressures, while RO membrane has the lowest flux. The pure water permeabilities as calculated from Eq. (4) were 6.30, 4.16, and 1.20 $Lh^{-1}m^{-2}bar^{-1}$ (63.0, 41.6, 12.0 L $h^{-1}m^{-2}MPa^{-1}$) for NF99, DK, and RO membranes, respectively. The gap in water flux value is cleared between RO and NF membranes.

Effect of Pressure on Rejection of Main Components Dissolved in AMD and Flux

This section will present the effect of pressure on rejection of main components dissolved in AMD and permeate flux using all investigated membranes at the two studied concentration levels; low and high concentrations of synthetic AMD (Table 1). The rejection of the main components dissolved in AMD will be considered as the total rejection based on the electrical conductivity of feed and permeate of AMD solution and as rejection of all toxic metals, and the rejection of sulphate ion involved in the AMD solution. The pressure spans the range of 5 to 20 bar (0.5 to 2 MPa) at a feed flow rate of 600 L/h, temperature of 20°C, and pH of 2.4.

Low Concentration Level

Figures 3(a–c) show the rejection of ions dissolved in synthetic AMD at low concentration level based on the electrical conductivity as well as the rejection of each metal
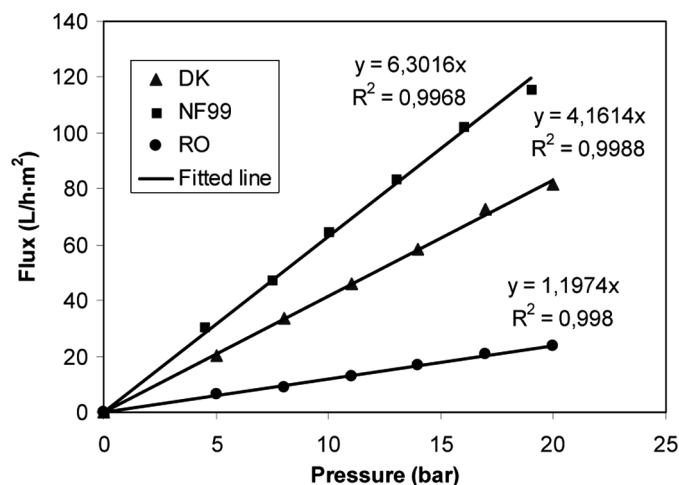

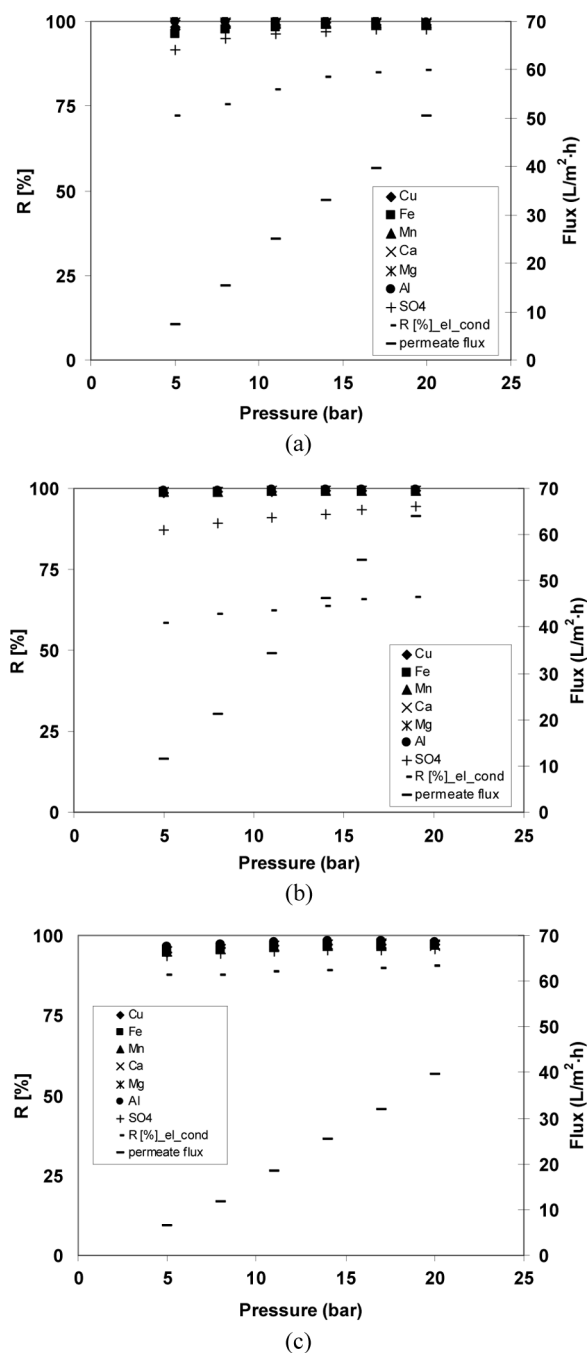FIG. 2.   Pure water permeability for three investigated membranes.

FIG. 3. Effects of pressure on metals and sulphate rejections and permeate flux at low concentration level for the investigated membranes (a) DK, (b) NF99, and (c) RO.

found in AMD and sulphate ion for all studied membranes with different pressure. It is clear that rejection of all metals is very high (>98%) and almost constant with increasing pressure for all investigated membranes except RO. At low pressure, the rejection of each metal using RO is relatively low (94%) as shown in Fig. 3(c). The high values of NF, which are promising for use in the AMD

treatment, could be explained on the basis of steric hindrance mechanism due to the fact that NF membranes have relatively small pore size in comparison to the metal size (30). For RO, the rejection of ions results from their diffusion through the membrane. On the other hand, rejection of sulphate and the rejection based on the electrical conductivity are clearly increased with increasing pressure for all membranes under study. Both DK and RO have high rejection (>92%) of sulphate ion over the range of pressure under investigation, while NF99 has relatively low rejection (85%) as shown in Fig. 3(b). For the rejection based on the electrical conductivity, RO has relatively high rejection compared to the rejection obtained using other membranes. On the other hand, the relations between the permeate flux of synthetic AMD at low concentration level and pressure for the three membranes under study are presented on the right axis of Figs. 3(a–c). It can be seen from these figures that increase in pressure leads to increase in permeate flux, a fact which can be interpreted in view of the increase in solvent flux. The use of NF99 leads to relatively high flux ($67\,\mathrm{L/m^2\cdot h}$ at 20 bar; (2 MPa)) as shown in Fig. 3(b) compared to the flux ($50\,\mathrm{L/m^2\cdot h}$ at 20 bar (2 MPa)) as obtained using a DK membrane as shown in Fig. 3(a). RO provides the lowest flux ($39\,\mathrm{L/m^2\cdot h}$ at 20 bar (2 MPa)) among the studied membranes as shown in Fig. 3(c) indicating inappropriateness of RO in the treatment of this type of wastewater in comparison to NF membranes.

High Concentration Level

The rejection of the main components dissolved in AMD based on electrical conductivity as well as the permeate flux at high concentration level for all studied membranes with different pressures are shown in Figs. 4(a–c). This will address the concentration effect on the rejection and permeate flux of all membranes under study. Again, the effect of pressure on the rejection of all investigated metals is constant for DK and RO as shown in Figures 4(a,c), while for NF99 the rejection is slightly increased with increasing pressure as shown in Fig. 4(b). The sulphate rejection for DK and NF99 at high concentration level has a similar trend as the rejection of sulphate at low concentration. RO is clearly affected by the concentration of sulphate as presented in Fig. 4(c), whereas its rejection is decreased at high concentration level. This could be explained by the increase of osmotic pressure for all membranes under investigation. In addition, the rejection of the main components dissolved in AMD based on electrical conductivity is slightly decreased at the high concentration level for all membranes under study. On the other hand, the effect of concentration of AMD on permeate flux becomes visible on Figs. 4 (a–c) where its value is lower at high concentration than at low concentration. Again, NF has the highest flux while RO has the lowest flux among the investigated membranes. It is worth
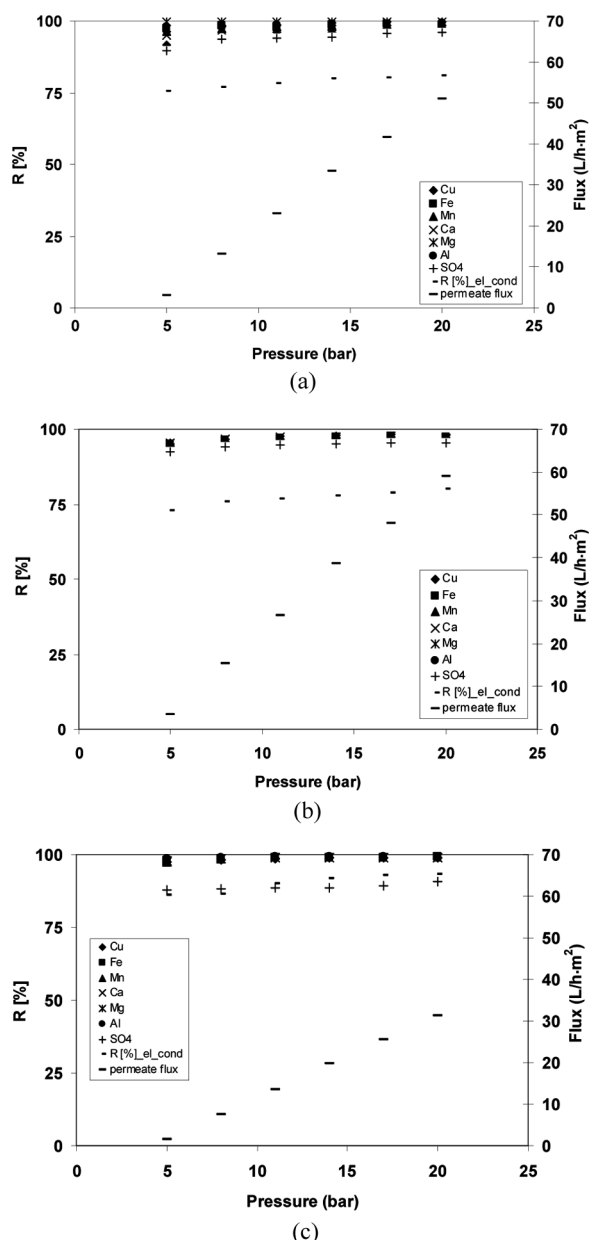
FIG. 4. Effects of pressure on metals and sulphate rejections and permeate flux at high concentration level for the investigated membranes (a) DK, (b) NF99, and (c) RO.

mentioning that NF membranes are preferable over RO in treating AMD due to their high rejection and permeate flux. Moreover, NF systems require a lower operating pressure range than RO, making energy costs and the overall process costs are satisfactorily lower by about 25%.

Effect of Feed Flow Rate on Rejection of Main Components Dissolved in AMD and Flux

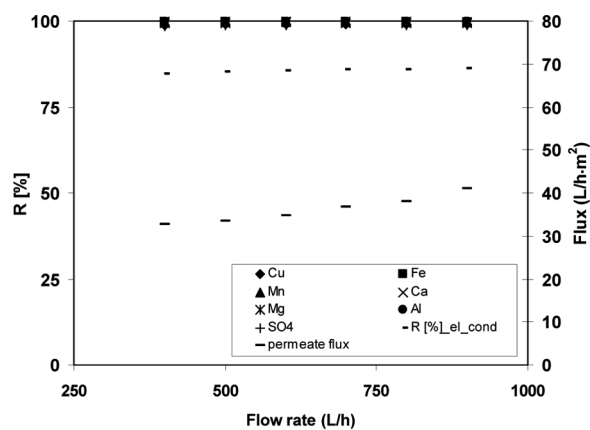The effect of feed flow rate on the rejection of main components dissolved in AMD and permeate flux using all investigated membranes at the two studied concentration levels is studied in this section. The value of the studied feed flow rate is in the range of 900 to 400 L/h at pressure of 15 bar (1.5 MPa), 20°C, and pH of 2.4.
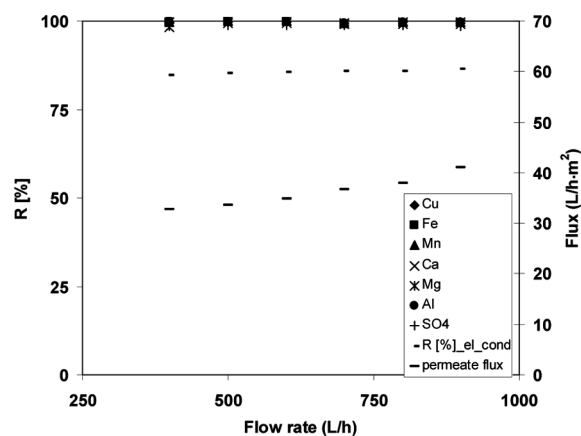
Low Concentration Level

Figures 5(a–c) present the relation of the rejection of main components dissolved in AMD at low concentration level based on the electrical conductivity as well as the rejection of each metal ion and sulphate ion for all studied membranes and values of the feed flow rate. Over the studied values of the flow rate, it is clear, that their effect on all rejection types is negligible. Moreover, the rejection of all metals is very high (>99%) for all investigated membranes as shown in Figs. 5(a–c). Both DK and RO have a high rejection of sulphate (97%) and rejection of the main components dissolved in AMD based on electrical conductivity (85% for DK, and 91% for RO). However, NF99 has relatively low rejection values of 94% and 72% of sulphate and total rejection based on electrical conductivity respectively. A significant increase in permeate flux with increasing feed flow rate for all studied membranes is clearly shown on the latter figures. The highest flux was obtained by NF99, while RO has the lowest flux among the studied membranes. Therefore, it is recommended to use the feed flow rate at high value as much as possible, as its value affects the permeate flux. This will depend on the system design of the membrane cell and the available energy. Of course a higher feed flow rate causes higher energy input, but also reduces the scaling risk because of higher shear forces at the membrane surface. Experimental investigations must be performed here, to find the most optimal flow rate – energy ratio for the used process design for any single case.
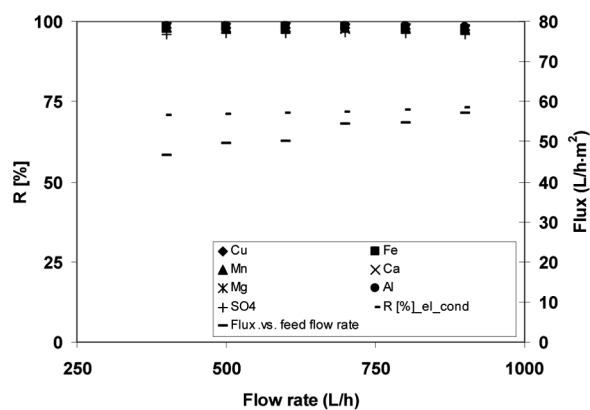
High Concentration Level

The effect of concentration on all types of rejection and permeate flux at different feed flow rate will be considered in this section. Figures 6(a–c) show the relation of the rejection of the main components dissolved in AMD and total rejection based on electrical conductivity at a high concentration level for all investigated membranes. Again, there is no effect of the feed flow rate on all types of rejections for all studied membranes. Moreover, the rejection at high concentration level has similar values at low concentration, which potentially confirms that membranes are suitable to treat AMD even at severe conditions. However, the effect of concentration on permeate flux at different flow rate is clearly shown in the right axes of Figs. 6(a–c). It has been observed that the permeate flux decreases with increasing concentration of AMD and decrease of feed flow rate for all studied membranes. In more details, the flux is dramatically increased at high flow rate (>600 L/h) for NF membranes as presented in Figs. 6(a–b), while for RO it
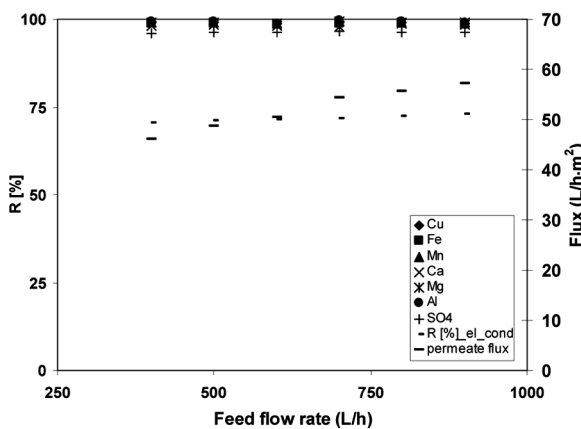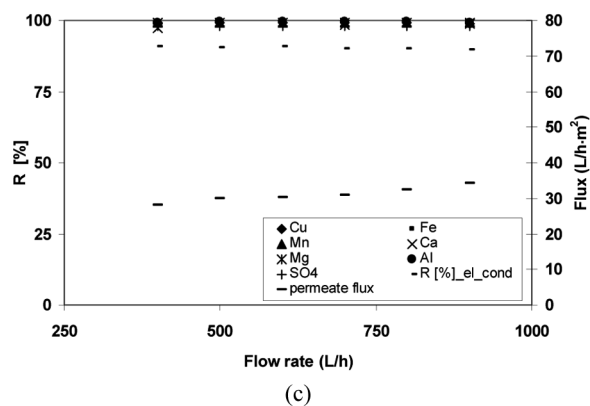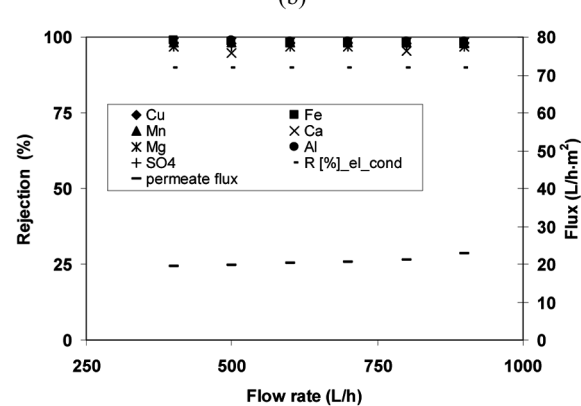
FIG. 5.   Effects of feed flow rate on metals and sulphate rejections and permeate flux at low concentration level for the investigated membranes (a) DK, (b) NF99, and (c) RO.

FIG. 6.   Effects of feed flow rate on metals and sulphate rejections and permeate flux at high concentration level for the investigated membranes (a) DK, (b) NF99, and (c) RO.

is slightly increased (almost constant) with increasing flow rate as shown in Fig. 6 (c). These results can be explained by the influence of the feed flow rate on the boundary layer at the membrane surface—increasing feed flow rate causes a reduction of the boundary layer thickness, which causes a reduction of the mass transfer resistance, subsequently followed by higher permeation (44).

Effect of Temperature on Rejection of Main Components Dissolved in AMD and Flux

Studying the temperature factor is very crucial in this study for the reason that some applications of membrane technology at elevated temperature take place in many industries such as mining industry, pulp and paper industry,

sugar industry, and textile industry (34,45). Therefore, the effect of temperature on the rejection and permeate flux has been investigated in this work in the range of 20 to 60°C at a pressure of 15 bar (1.5 MPa), feed flow rate of 600 L/h, and pH of 2.4. The temperature was chosen in this range so its value does not exceed the maximum temperature suggested by the membrane manufacturers as shown in Table 2.

Low Concentration Level

All investigated rejection types as a function of temperature at low concentration level using the three investigated membranes will be considered in this section. The total rejection of the main components dissolved in AMD based on electrical conductivity and the rejection of metal ions, as well as the rejection of sulphate ion, are shown in Figs. 7(a–c) for the investigated membranes. The rejection of metals and sulphate are slightly decreased with increasing temperature, while the rejection based on electrical conductivity is dramatically decreased with temperature as shown in Figs. 7(a–b). This can be interpreted due to variations in NF membrane properties such as the effective intra-pore solute diffusivity, the membrane pore radius, or effective thickness (35,46). Another significant reason is the change of the charge of the active layer of NF membranes with temperature (36). On the other hand, all types of rejection are not affected by an increase of the temperature for RO as shown in Fig. 7(c). This confirmed that the surface of RO does not contain any charge on its active layer which may change the separation performance of RO. Therefore, RO seems to be preferable to NF in the treatment of AMD at high temperature. The permeate flux is also studied with temperature and it is shown in the right axis of Figs. 7(a–c). It is evident that the flux increased with increasing temperature for all investigated membranes due to the decrease in viscosity of AMD as well as increase in the kinetic energy of AMD. NF99 has the highest flux among the investigated membranes especially at high temperature as shown in Fig. 7(b) while RO has the lowest flux. It thus concludes that RO membranes have the potential to be used in the treatment of AMD at high temperature with medium permeate flux.

High Concentration Level

Figures 8(a–c) present all types of rejection with temperature for all studied membranes at high concentration level. Temperature has a significant effect on the rejection of the sulphate ion for NF membranes as shown in Figs. 8(a–b) while for RO the sulphate rejection was almost constant with temperature as shown in Fig. 8(c). Again, the rejection of metals as well as the total rejection of the main components dissolved in AMD based on electrical conductivity is decreased with temperature. Moreover, a significant increase in flux with temperature is cleared in Figs. 8(a–c) for all studied membranes.
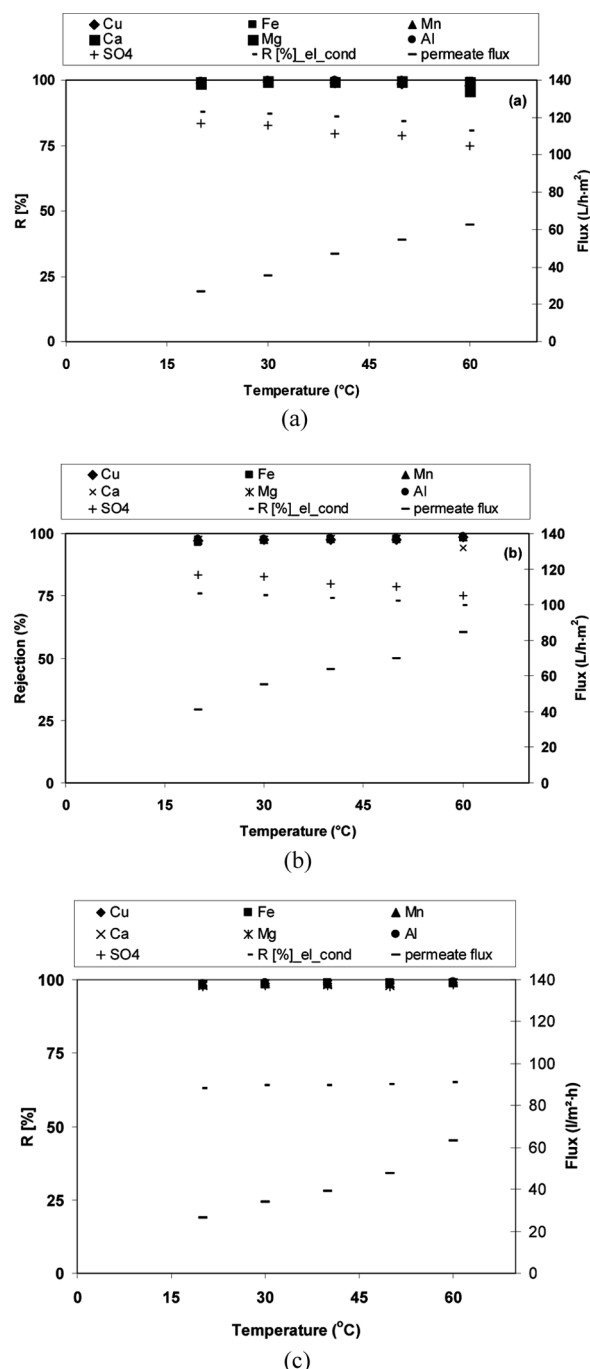

FIG. 7. Effects of temperature on metals and sulphate rejections and permeate flux at low concentration level for the investigated membranes (a) DK, (b) NF99, and (c) RO.

Large-Scale Results

The filtration of synthetic AMD at high concentration level has only been conducted using NF99 in large-scale experiments (i.e., area $6 m^2$). This will check the applicability of membrane technology on treatment of AMD at commercial scale. In this case, the studied parameters
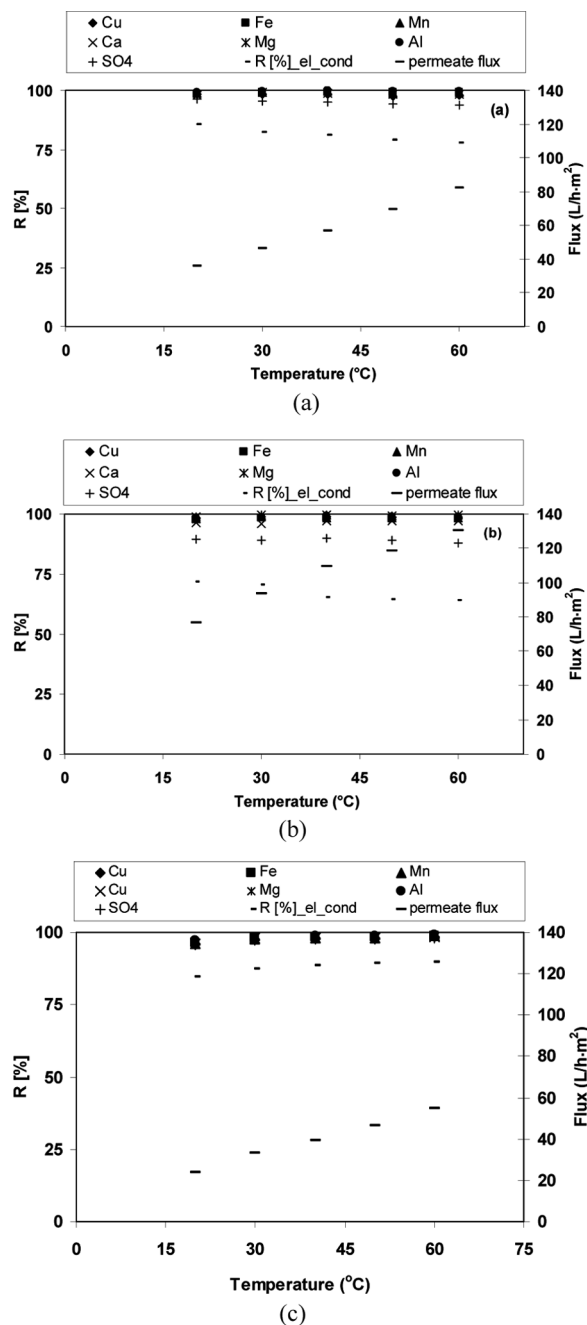
(a)

(b)

(c)

FIG. 8. Effects of temperature on metals and sulphate rejections and permeate flux at high concentration level for the investigated membranes (a) DK, (b) NF99, and (c) RO.
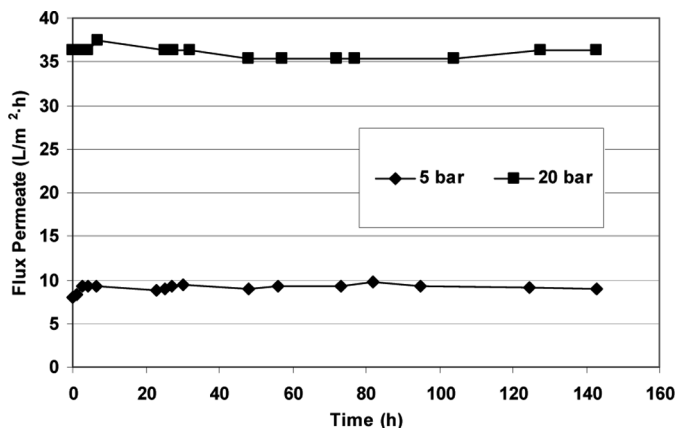
FIG. 9. Effect of pressure and time on permeate flux of AMD using NF99 at temperature of 20°C, pH of 2.4, and feed flow rate of 1000 l/h.

higher value (36 L/m².h) at 30 bar (3 MPa) than the value (9 L/m².h) at 5 bar (0.5 MPa), which is the same finding obtained in small-scale experiments. Based on a filtration area of 6 m² for the commercial scale test and a feed flow rate of 1000 l/h as done in this test, the recovery calculates from about 22% to about 6% depending on the pressure. It is clear, that with a higher filtration area, a higher recovery is possible. The effect of pressure on the rejection of AMD is also investigated at different pressures (10, 20, and 30 bar (1, 2 and 3 MPa)) and at high acidity (pH = 1.5) and is shown in Fig. 10. It is clear that NF99 shows its ability to reject both metals at high values (>98%) and sulphate rejection at moderate values (86%), which confirms its suitability in the treatment of this type of wastewater even at low pressure (10 bar (1 MPa)) and pH of 1.5. In addition, the effect of pressure is clearly weak on the rejection of the main components dissolved in AMD, which caused the operation of the NF cell at a pressure higher than 10 bar (1 MPa) is not necessary. Finally, the effect of pH on the performance of NF99 in the treatment of AMD has been studied and shown

FIG. 10. Effect of pressure on the rejection of ions involved in the high concentration of AMD using NF99 at temperature of 20°C, pH of 1.5, and feed flow rate of 800 l/h.

investigated are pressure, time, and pH. Figure 9 shows the effect of time on permeate flux at pressure of 5 and 20 bar (0.5 and 2 MPa). For each pressure, the flux was measured for experiment duration in the range of 0 to 143 hour at a temperature of 20°C, pH of 2.4, and feed flow rate of 1000 L/h. It is elucidated, that the flux decline is very low indicating the neglected scaling effect on the membranes surface at the studied conditions. Moreover, the flux has a
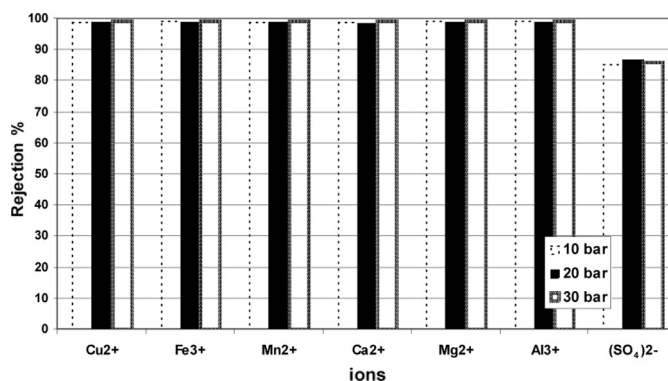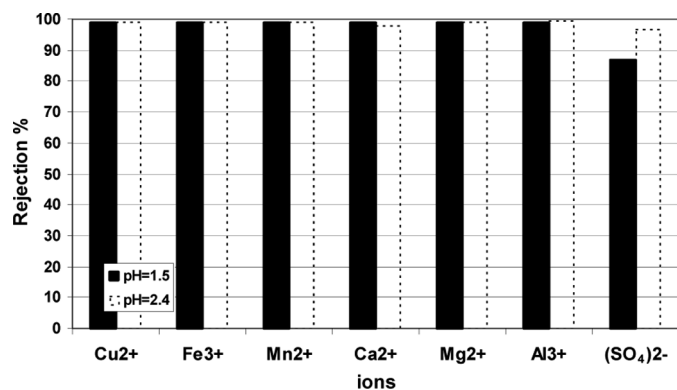
FIG. 11. Effect of pH on the rejection of ions involved in the high concentration of AMD using NF99 at temperature of 20°C, pressure of 20 bar, and feed flow rate of 800 l/h.

in Fig. 11. This figure shows that the rejection of all investigated ions is slightly decreased with decreasing pH except sulphate ion, which is clearly decreased at low pH. This can be interpreted by the fact that the surface charge of NF membranes becomes increasingly more negative as pH is increased (37,43). Accordingly, increasing the surface charge of the membrane results in increased electrostatic repulsion between a negatively charged sulphate ion and NF caused the increasing in rejection of the sulphate ion at a high pH.

CONCLUSION

To determine and optimize their suitability in an alternative treatment of AMD, three commercial membranes (DK, NF99, RO) were employed in a laboratory-scale study with membrane area of $63.6 \, cm^2$ to investigate their performance in handling synthetic AMD at two different concentration levels representing actual AMD concentration in the mining industry. Pressure, temperature, feed flow rate, and pH were the investigated parameters in this study. Moreover, this work studied the treatment of AMD using NF99 at large scale with membrane area of about $6 \, m^2$ in order to check the applicability of this treatment at a commercial scale.

PHREEQC was used in this work to determine the scaling risk in the prepared AMD at the typical conditions of the preparation. The results showed that rejection of the main components dissolved in AMD is slightly affected with increasing pressure, while the effect of feed flow rate is negligible for all investigated membranes. However, the rejection of the main components dissolved in AMD significantly decreased with increasing temperature for NF membranes at two concentration levels. For RO, the rejection was constant even at high temperature which caused RO to be preferable over the NF membranes at the latter condition. The results also showed that NF99 has the highest flux among the investigated membranes while RO has

the lowest flux. Therefore, NF membranes are more suitable than RO in AMD treatment at a relatively low temperature due to their high flux and rejections.

ACKNOWLEDGEMENTS

REFERENCES

1. Younger, P.; Banwart, S.; Hedin, R. (2002) Mine water chemistry. In: *Mine Water: Hydrology, Pollution, Remediation,* Ch. 2. Springer-Verlag, New York, LLC, pp. 65–126.
2. Gitari, M.; Petrik, L.; Etchebers, O.; Key, D.; Iwuoha, E.; Okujeni, C. (2006) Treatment of acid mine drainage with fly ash: Removal of major contaminants and trace elements. *J. Environ Sci. Health-Part A*, A41 (8): 1729.
3. Nordstrom, D.K.; Alpers, Ch.N.; Ptacek, C.J.; Blowes, D.W. (2000) Negative pH and extremely acidic mine waters from Iron Mountain, California. *Environmental Science & Technology*, 34: 254–258.
4. Akcil, A.; Koldas, S. (2006) Review article: Acid Mine Drainage (AMD): Causes, treatment and case studies. *J. Cleaner Production*, 14: 1139.
5. Lyew, D.; Knowles, R.; Sheppard, J. (1994) The biological treatment of acid mine drainage under continuous flow conditions in a reactor. *Trans IChemE*, 72 (B): 42.
6. Hedin, R.; Watzlaf, G.; Nairn, R. (1994) Passive treatment of acid mine drainage with limestone. *J. Environ. Qual.*, 23: 1338.
7. Dempsey, B.; Jeon, B. (2001) Characteristics of sludge produced from passive treatment of mine drainage. *Geochem. Explor. Environ. Anal.*, 1: 89.
8. Sibrell, P.; Watten, B.J. (2003) Evaluation of sludge produced by limestone neutralization of AMD at the Friendship Hill National Historic Site. In: *Proceedings of the 20th Annual Meeting American Society for Mining and Reclamation*, Billings, Montana, pp. 1151–1169.
9. Santomartino, S.; Webb, J. (2007) Estimating the longevity of limestone drains in treating acid mine drainage containing high concentrations of iron. *Applied Geochemistry*, 22: 2344.
10. Smith, P.; Hancoc, S. (1992) Brukunga - The acid test. Waste Disposal and Water Management in Australia, December, pp. 3–11.
11. Igarashi, T.; Asakura, K.; Yoshida, T.; Miyamae, H.; Iyatomi, N.; Hashimoto, K. (2006) Ferrite formation using precipitate in the treatment of acid mine drainage for reducing its volume. In: *Proceedings of the 5th International Congress on Environmental Geotechnics*, Cardiff, Wales, UK, pp. 909–916.
12. Herrera, S.; Uchiyama, H.; Igarashi, T.; Asakura, K.; Ochi, Y.; Ishizuka, F.; Kawada, S. (2007) Acid mine drainage treatment through a two-step neutralization ferrite-formation process in northern Japan: Physical and chemical characterization of the sludge. *Minerals Engineering*, 20: 1309.
13. Feng, D.; van Deventer, J.; Aldrich, C. (2004) Removal of pollutants from acid mine wastewater using metallurgical byproduct slags. *Separation and Purification Technology*, 40: 61.
14. Petrik, L.; White, R.; Klink, M.; Somerset, V.; Burgers, C.; Frey, M. (2003) Utilisation of South African fly ash to treat acid mine drainage, and production of high quality zeolites from the residual solids. In: *Proceedings of the 2003 International Ash Utilisation Symposium*, University of Kentucky, USA, Paper no. 61.
15. Maree, J.P.; Hlabela, P.; Negovhela, R.; Geldenhuys, A.J.; Mbhele, N.; Nevhulaudzi, T.; Waanders, F.B. (2004) Treatment of Mine Water for sulphate and metal removal using Barium sulphide. *Mine Water and the Environment*, 23: 195–203.

16. Rıos, C.; Williams, C.; Roberts, C. (2008) Removal of heavy metals from acid mine drainage (AMD) using coal fly ash, natural clinker and synthetic zeolites. *J. Hazardous Materials*, 156: 23.

17. Gitari, W.; Petrik, L.; Etchebers, O.; Key, D.; Iwuoha, E.; Okujeni, C. (2008) Passive neutralisation of acid mine drainage by fly ash and its derivatives: A column leaching study. *Fuel*, 87: 1637.

18. Potgieter-Vermaak, S.; Potgieter, J.; Monama, P.; Van Grieken, R. (2006) Comparison of limestone, dolomite and fly ash as pre-treatment agents for acid mine drainage. *Minerals Engineering*, 19: 454.

19. Cheong, Y.; Min, J.; Kwon, K. (1998) Metal removal efficiencies of substrates for treating acid mine drainage of the Dalsung mine, South Korea. *J. Geochemical Exploration*, 64: 147.

20. Peppas, A.; Komnitsas, K.; Halikia, I. (2000) Use of organic covers for acid mine drainage control. *Minerals Engineering*, 13 (5): 563.

21. Tuttle, J.; Dugan, P.; Macmillan, C.; Randle, C. (1969) Microbial dissimilatory sulfur cycle in acid mine water. *J. Bacteriol*, 97: 594.

22. Wildeman, T.; Laudon, L. (1989) The Use of Wet-lands for Treatment of Environmental Problems in Mining: Non-coal Mining Applications. In: *Proceedings of the International Conference on Constructed Wetlands for Wastewater Treatment*, ed., Hammer, D.H., Lewis Publishing: Ann Arbor, MI., pp. 221–231.

23. Ueki, K.; Ueki, A.; Itoh, K.; Tanaka, T.; Satoh, A. (1991) Removal of sulfate and heavy metals from acid mine water by anaerobic treatment with cattle waste: Effects of heavy metals on sulfate-reduction. *J. Environ. Sci. Health A*, 26 (8): 1471.

24. Wakao, N.; Takahashi, T.; Sakurai, Y.; Shiota, H. (1979) A treatment of acid mine water using sulfate- reducing bacteria. *J. Fermentation Technol.*, 57 (5): 445.

25. Dvorak, D.; Hedin, R.; Edenborn, H.; McIntire, P. (1992) Treatment of metal-contaminated water using bacterial sulfate reduction: Results from pilot-scale reactors. *Biotech. Bioeng.*, 40: 609.

26. Barnes, L.; Janssen, F.; Scheeren, P.; Versteegh, J.; Koch, R. (1992) Simultaneous microbial removal of sulfate and heavy metals from waste water. *Trans. Inst. Min. Metall. C*, 101: 181.

27. Riveros, P. (2004) The extraction of Fe(III) using cation-exchange carboxylic resins. *Hydrometallurgy*, 72: 279.

28. Al-Zoubi, H.; Steinberger, P.; Pelz, W.; Haseneder, R.; Härtel, G. (2009) Nanofiltration of acid mine drainage. *Journal of Desalination and Water Treatment*, (in press).

29. Hilal, N.; Al-Zoubi, H.; Darwish, N.; Mohammed, A.; Abu Arabi, M. (2004) A comprehensive review of nanofiltration membranes: Treatment, pretreatment, modelling, and atomic force microscopy. *Desalination*, 170: 281.

30. Hilal, N.; Al-Zoubi, H.; Mohammad, A.W.; Darwish, N.A. (2005) Nanofiltration of highly concentrated salt solutions up to seawater salinity. *Desalination*, 184: 315–326.

31. Al-Zoubi, H.; Hilal, N.; Darwish, N.A.; Mohammad, A.W. (2007) Rejection and modelling of sulphate and potassium salts by nano-filtration membranes: Neural network and Spiegler–Kedem model. *Desalination*, 206: 42–60.

32. Al-Zoubi, H.; Omar, W. (2009) Rejection of salt mixtures from high saline by nanofiltration membranes. *Korean Journal of Chemical Engineering*, 26 (3): 799–805.

33. Hilal, N.; Al-Zoubi, H.; Darwish, N.; Mohammad, A.W. (2007) Performance of nanofiltration membranes in the treatment of synthetic and real seawater. *Separation Science and Technology*, 42 (3): 493–515.

34. Snow, M.J.; deWinter, D.; Buckingham, R.; Campbell, J.; Wagner, J. (1996) New techniques for extreme conditions: High temperature reverse osmosis and nanofiltration. *Desalination*, 105: 57–61.

35. Nilsson, M.; Tragardh, G.; Stergren, K. (2006) The influence of sodium chloride on mass transfer in a polyamide nanofiltration membrane at elevated temperatures. *J. Membr. Sci.*, 280: 928.

36. Nilsson, M.; Lipnizki, F.; Tragardh, G.; Stergren, K. (2008) Performance, energy and cost evaluation of a nanofiltration plant operated at elevated temperatures. *Separation and Purification Technology*, 60: 36–45.

37. Hagmeyer, G.; Gimbel, R. (1998) Modelling the salt rejection of nanofiltration membranes for ternary ion mixtures and for single salts at different pH values. *Desalination*, 117: 247–256.

38. Deshmukh, S.S.; Childress, A.E. (2001) Zeta potential of commercial RO membranes: Influence of source water type and chemistry. *Desalination*, 140: 87–95.

39. Murthy, Z.V.P.; Chaudhari, L.B. (2009) Separation of binary heavy metals from aqueous solutions by nanofiltration and characterization of the membrane using Spiegler–Kedem model. *Chemical Engineering Journal*, 150: 181–187.

40. Parkhurst, D.L.; Appelo, C.A.J. (2003) PHREEQC (Version 2)-A Computer Program for Speciation, Batch-Reaction, One-Dimensional Transport, and Inverse Geochemical Calculations. Software-Version 2.16.03.

41. Parkhurst, D.L.; Appelo, C.A.J. (1999) User's guide to PHREEQC (Version 2)—a computer program for speciation, batch-reaction, one-dimensional transport, and inverse geochemical calculations. U.S. Geological Survey Report no. 99–4259, Denver, Colorado 326 pp.

42. Stumm, W.; Morgan, J.J. (1996) *Aquatic Chemistry – Chemical Equilibria and Rates in Natural Waters.* 3rd Edition, Wiley Interscience Series of Texts and Monographs: New York.

43. Lee, S.; Park, G.; Amy, G.; Hong, S.K.; Moon, S.H.; Lee, D.H.; Cho, J. (2002) Determination of membrane pore size distribution using the fractional rejection of non-ionic and charged macromolecules. *J. Membr. Sci.*, 201: 191–201.

44. Rieger, A.; Steinberger, P.; Pelz, W.; Haseneder, R.; Härtel, G. (2009) Mine water treatment by membrane filtration processes – Experimental investigations on applicability. *Journal of Desalination and Water Treatment*, 6: 54–60.

45. Chen, Ci.; Chai, X.; Yue, P.L.; Mi, Y. (1997) Treatment of textile desizing wastewater by pilot scale nanofiltration membrane separation. *J. Membr. Sci.*, 127: 93–99.

46. Ben Amar, N.; Saidani, H.; Palmeri, J.; Deratani, A. (2006) Temperature dependence of water and neutral solutes transport in nanofiltration membranes. *Desalination*, 199: 46–48.